

Anomalous pseudogap in population imbalanced Fermi superfluids

Madhuparna Karmakar and Pinaki Majumdar

Harish-Chandra Research Institute, Chhatnag Road, Jhansi, Allahabad 211 019, India

(Dated: October 23, 2018)

In a Fermi superfluid increasing population imbalance leads initially to reduction of the transition temperature, then the appearance of modulated Fulde-Ferrell-Larkin-Ovchinnikov (FFLO) states, and finally the suppression of pairing itself. For interaction strength such that the ‘balanced’ system has a normal state pseudogap, increasing imbalance reveals anomalous spectral behavior. At a fixed weak imbalance (small polarization) the stable homogeneous superfluid occurs only above a certain temperature. The density of states has a minimum at the Fermi level, then a weak peak *within the gap*, and then the large, gap edge, coherence features. On heating, this non monotonic energy dependence changes to a more conventional fluctuation driven pseudogap, with a monotonic energy dependence. At large imbalance the ground state is FFLO and ‘pseudogapped’ due to the modulated order. It changes to a gapless normal state on heating, and then shows a pseudogap again at a higher temperature. These weak imbalance and strong imbalance features both involve effects well beyond mean field theory. We establish them by using a Monte Carlo technique on large lattices, motivate the results in terms of the pairing field distribution, and compare them to spectroscopic results in the imbalanced unitary Fermi gas.

I. INTRODUCTION

Attractive interaction between fermions lead to pairing and a superfluid or superconducting ground state. If the interaction strength is large the pairing effects show up at a high temperature, T_{pair} , via a pseudogap in the density of states, while the transition to a superfluid occurs at a lower temperature T_c . Between T_{pair} and T_c the pseudogap deepens and for $T \lesssim T_c$ one expects a full gap in the density of states. The loss in low energy spectral weight with reducing temperature is monotonic¹.

Since the pairing occurs between time reversed states $\mathbf{k} \uparrow$ and $-\mathbf{k} \downarrow$ an imbalance in the population of the ‘up’ and ‘down’ species, with the total fixed, tends to reduce the pairing amplitude and the T_c . The imbalance can be achieved by applying a magnetic field, as in the solid state², or by loading different numbers of up and down fermions into a trap - as in cold atom experiments³⁻⁵.

The effect of increasing field, h , or growing population imbalance, P , is qualitatively similar: it suppresses the T_c of the homogeneous superfluid (SF), promotes a ‘phase modulated’ Fulde-Ferrell (FF) or an ‘amplitude modulated’ Larkin-Ovchinnikov (LO) state in the intermediate P regime, and finally destroys pairing altogether⁶⁻⁸. There are also crucial differences. For example, while there is a stable ground state for *all applied fields*, there is no stable ground state for polarization $0 < P < P_{c1}$, where P_{c1} is the threshold polarization of the FFLO state. At zero temperature the system can either be an unpolarised (homogeneous) superfluid (USF) with $P = 0$, or a modulated state with $P_{c1} \leq P \leq P_{c2}$, or a homogeneous ‘normal’ state with $P > P_{c2}$. There is an unstable (phase separation) window $0 < P < P_{c1}$. This window shrinks with increasing temperature vanishing at a tricritical point. The general features are well understood theoretically⁹⁻¹² and have been verified in cold Fermi gases at unitarity^{3,13}.

What is less well known is the changing spectral character of the imbalanced SF with increasing temperature. We establish this for the two dimensional attractive Hubbard model at intermediate coupling, where the T_c is highest, using a Monte Carlo approach. We discover the following:

1. At low imbalance the homogeneous superfluid is stable only above some temperature $T_{un}(P)$ and for $T \gtrsim T_{un}$ has a pseudogap with a strange non monotonic low energy density of states. Heating this leads to a crossover to a more conventional pseudogap phase with a monotonic energy dependence.
2. For $P > P_{c1}$, where the ground state is FFLO, increasing temperature generates multiple crossovers: from the ‘pseudogapped’ FFLO to a gapless normal state, and, beyond a higher temperature, to another pseudogapped normal state.
3. The non paired ground state, with $P > P_{c2}$, is gapless but on heating develops a weak pseudogap beyond a certain temperature. This phase is observed in a situation where there is no order at any temperature, *i.e.*, $T_c = 0$.

II. MODEL AND METHOD

We study the attractive two dimensional Hubbard model on a square lattice in the presence of a magnetic field:

$$H = H_0 - h \sum_i \sigma_{iz} - |U| \sum_i n_{i\uparrow} n_{i\downarrow} \quad (1)$$

with, $H_0 = \sum_{ij,\sigma} (t_{ij} - \mu \delta_{ij}) c_{i\sigma}^\dagger c_{j\sigma}$, where $t_{ij} = -t$ only for nearest neighbor hopping and is zero otherwise. $\sigma_{iz} = (1/2)(n_{i\uparrow} - n_{i\downarrow})$. We will set $t = 1$ as the reference energy scale. μ is the chemical potential and h is the applied magnetic field in the \hat{z} direction. $U > 0$ is the strength of on-site attraction. We will use $U/t = 4$ and $\mu = -0.2t$ ($n \sim 0.94$).

We have discussed our method of solving the model in detail elsewhere^{14,15} so we touch on it only briefly. We use a ‘single channel’ Hubbard-Stratonovich (HS) decomposition of the interaction in terms of an auxiliary complex scalar field $\Delta_i(\tau) = |\Delta_i(\tau)| e^{i\theta_i(\tau)}$. This maps the original interacting problem to that of non interacting fermions in a space-time

fluctuating field $\Delta_i(\tau)$, the price to pay is the additional ‘averaging’ over all configurations of $\Delta_i(\tau)$. Quantum Monte Carlo performs this averaging without further approximation, mean field theory (MFT) restricts $\Delta_i(\tau)$ to a time independent spatially periodic function, and dynamical mean field theory (DMFT) treats $\Delta_i(\tau)$ as a ‘single site’ time dependent function $\Delta(\tau)$.

We drop the ‘time’ dependence of Δ , but retain the full spatial dependence: $\Delta_i(\tau) \rightarrow \Delta_i$. This corresponds to dropping quantum fluctuations but retaining all the classical thermal fluctuations. Equivalently one can think of Fourier transforming the $\Delta_i(\tau)$ into bosonic Matsubara modes $\Delta_i(\Omega_n)$ and our approach corresponds to retaining the $\Omega_n = 0$ mode. This has been called a ‘static path approximation’ (SPA)^{16,17} to the functional integral for the partition function.

SPA retains classical fluctuations of arbitrary magnitude, around the saddle point, but no quantum ($\Omega_n \neq 0$) fluctuation. At $T = 0$, since the classical fluctuations die off, SPA reduces to standard Bogoliubov-de Gennes (BdG) mean field theory (MFT). For $T \neq 0$, however, it considers not only the saddle point configuration but *all* configurations involving classical amplitude and phase fluctuations of the order parameter. The BdG equations are solved in all these configurations to compute the thermally averaged properties. This approach suppresses the order parameter much quicker than MFT. Also, since the $\Omega_n = 0$ mode dominates the exact partition function, SPA becomes exact as $T \rightarrow \infty$. The approximation leads to the coupled equations:

$$H_{eff} = H_0 - h \sum_i \sigma_{iz} + \sum_i (\Delta_i c_{i\uparrow}^\dagger c_{i\downarrow}^\dagger + h.c.) + H_{cl}$$

$$P\{\Delta_i\} \propto Tr_{c,c^\dagger} e^{-\beta H_{eff}} \quad (2)$$

where $H_{cl} = \sum_i \frac{|\Delta_i|^2}{U}$ is the stiffness cost associated with the now classical auxiliary field. The upper equation describes fermions in a pairing background Δ_i , while the lower equation defines the probability distribution $P\{\Delta_i\}$ associated with a $\{\Delta_i\}$ configuration.

We generate samples of $\{\Delta_i\}$ using a Metropolis algorithm, diagonalising H_{eff} for the update cost. In order to make the study numerically less expensive the Monte Carlo is implemented using a cluster approximation¹⁸. After equilibration at a given h, T we calculate the following:

$$P(h, T) = \langle (1/N) \sum_i \langle n_{i\uparrow} - n_{i\downarrow} \rangle \rangle$$

$$S_{\mathbf{q}}(h, T) = \frac{1}{N^2} \sum_{i,j} \langle \Delta_i \Delta_j^* \rangle e^{i\mathbf{q} \cdot (\mathbf{r}_i - \mathbf{r}_j)}$$

$$N_{\uparrow}(\omega) = \langle (1/N) \sum_{i,n} |u_n^i|^2 \delta(\omega - E_n) \rangle$$

where $P(h, T)$ is the polarization (not be confused with the probability distribution of the pairing field discussed later), $S_{\mathbf{q}}(h, T)$ is the pairing structure factor, and $N_{\uparrow}(\omega)$ is the up spin density of states (DOS). The down spin DOS is symmetrically shifted. u_n^i are the usual BdG eigenfunctions and E_n are the BdG eigenvalues in an equilibrium configuration. Angular brackets indicate thermal average. Notice that the DOS

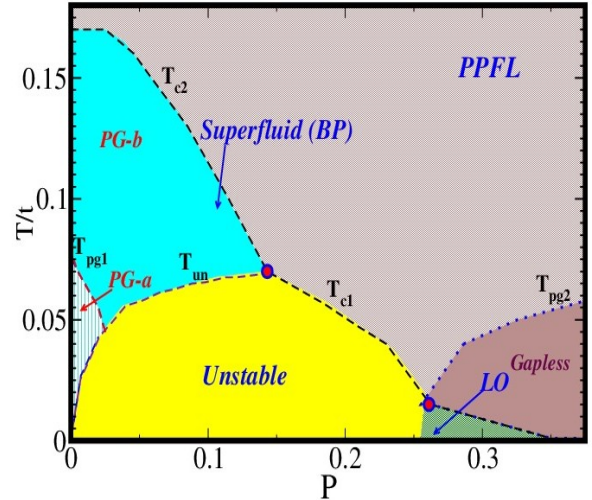


FIG. 1. The polarization (P) - temperature (T) phase diagram of the intermediate coupling attractive Hubbard model ($U = 4t$) and $n \sim 0.94$ in two dimensions. The thermodynamic phases include a homogeneous superfluid, FFLO states, a partially polarized Fermi liquid (PPFL), and an ‘unstable’ phase separated region. The spin resolved density of states can either have a hard gap, pseudogaps of different character, PG-a or PG-b (see text), or be gapless. The superfluid to PPFL transition is indicated as T_{c2} and T_{c1} , for 2nd and 1st order transitions respectively, and the unstable to superfluid boundary as T_{un} . The PG-a to PG-b crossover within the superfluid is denoted as T_{pg1} and the gapless to pseudogap crossover at large P denoted as T_{pg2} . The variation of T at fixed P can take the system through different pseudogap regimes.

is also the \mathbf{k} -summed spectral function $A_{\sigma}(\mathbf{k}, \omega)$. Formally,

$$A_{\sigma}(\mathbf{k}, \omega) = -(1/\pi) \text{Im} G_{\sigma}(\mathbf{k}, \omega)$$

with, $G_{\sigma}(\mathbf{k}, \omega) = \lim_{\eta \rightarrow 0} G_{\sigma}(\mathbf{k}, i\omega_n)|_{i\omega_n \rightarrow \omega + i\eta}$ where $G_{\sigma}(\mathbf{k}, i\omega_n)$ is the imaginary frequency transform of $\langle c_{\mathbf{k}\sigma}(\tau) c_{\mathbf{k}\sigma}^\dagger(0) \rangle$. The BdG quasiparticles are related to the original fermions via the eigenfunction matrix so the Green’s function and spectral functions can be readily computed¹⁹.

We wish to probe results at fixed P , for varying T , as would be the case in population imbalanced cold Fermi gases. Within the Hamiltonian formulation P is a derived quantity, dependent on h, T and the other model parameters. We therefore solve the $h - T$ problem first and then *construct* a $P - T$ phase diagram out of it.

Since mean field theory is widely used to study the imbalanced Fermi gas it is useful to point out that, apart from the gross overestimate of T_c , mean field theory predicts that the homogeneous SF is *always gapped*, and the normal state *always gapless*. The notion of a pseudogap does not figure in it¹.

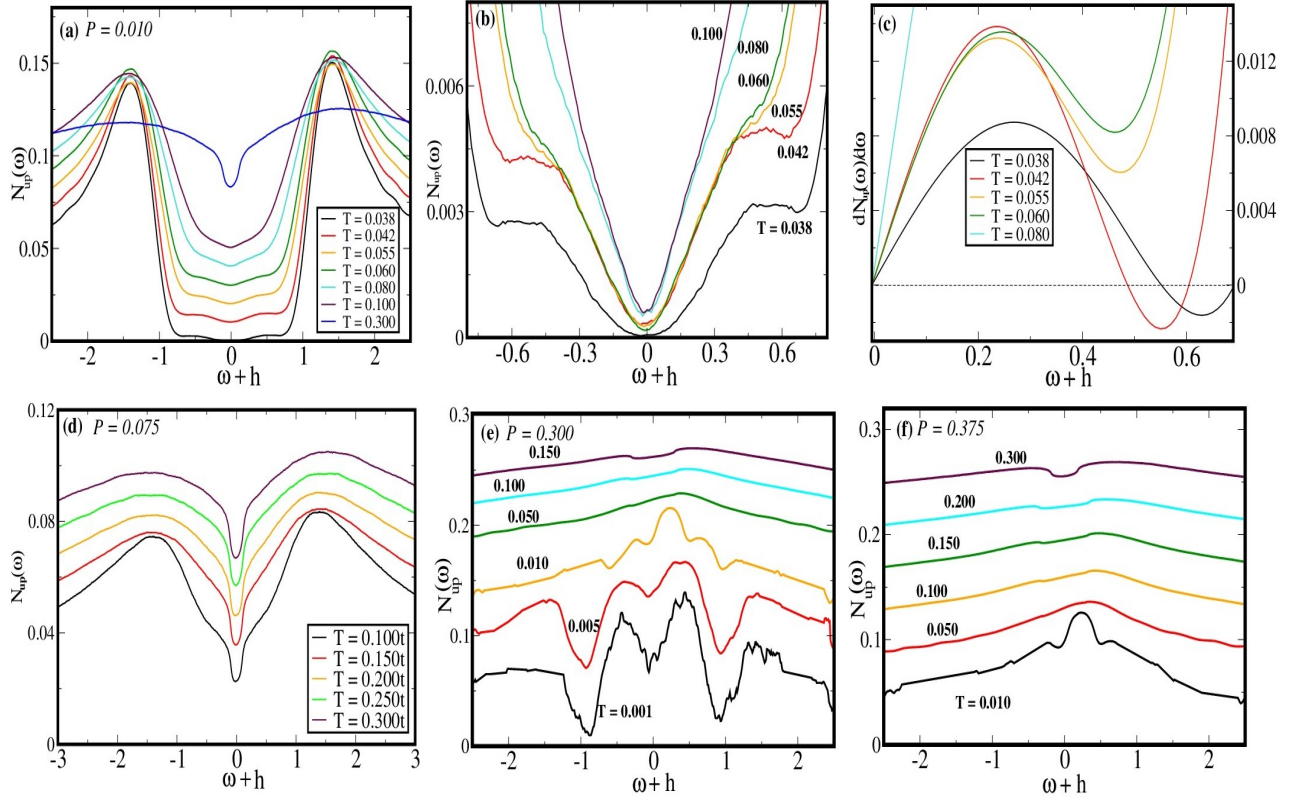


FIG. 2. Temperature dependence of the up spin DOS at (a) $P \sim 0.010$, (d) $P \sim 0.075$, (e) $P \sim 0.300$ and (f) $P \sim 0.375$. The plots are vertically shifted for clarity and the ω axis is shifted by $+h$ to center the gap feature on the origin. In (a) the DOS starts with PG-a character (see text) at the lowest accessible temperature, transforms to PG-b on heating (all within the SF phase), then to a pseudogapped normal state. In (d) the low T pseudogap weakens but persists across the SF to PPFL transition and on to high T . In (e) the ground state is ‘pseudogapped’ due to FFLO order. This is lost on transition to the PPFL but a weak PG reappears at high T . In (f) the PPFL ground state is gapless but develops a PG on heating. Panel (b) shows the DOS behavior at $P \sim 0.010$, focusing on the low energy window. Notice the change in character with increasing T . Panel (c) shows the energy derivative of the DOS at $P = 0.01$, the multiple changes in sign at low T indicate the multiple minima-maximum structure. The sign changes occur only for the two lowest T , which we have called the PG-a phase.

III. RESULTS

A. Phase diagram

Fig.1 shows the $P - T$ phase diagram inferred from the $h - T$ phase diagram (shown later, and also in ref.¹⁵). While the thermodynamic phase boundaries are determined based on $S_q(T)$, the various crossovers are determined based on the behavior of the DOS. A suppression in the density of states around the Fermi level (but not a hard gap) is characterized as a pseudogap (PG). In our case we classify the pseudogaps as PG-a and PG-b depending on the detailed spectral behavior in the subgap region. Considering the $\omega \geq 0$ window, PG-a has a minimum at $\omega = 0$, a local maximum at a low energy ω_{max} , a second minimum at an energy ω_{min} , say, and then the gap edge coherence features. PG-b involves a minimum only at $\omega = 0$. We first recapitulate the ground state then move to thermal properties.

1. Ground state:

In terms of an applied magnetic field, the ground state is a homogeneous unpolarised SF for fields $h < h_{c1} \sim 0.9t$. At h_{c1} it makes a transition to a finite polarization FFLO state, with $P = P_{c1}$. The FFLO regime is from h_{c1} to h_{c2} , with the polarization growing from P_{c1} to P_{c2} , and beyond h_{c2} the ground state has no pairing and is a partially polarized Fermi liquid (PPFL).

In terms of polarization, at $T = 0$ the entire $0 < h < h_{c1}$ region, with $P = 0$, collapses to the origin. The polarization regime $0 < P < P_{c1}$ is unstable, with no homogeneous phase allowed, followed by the FFLO and PPFL at higher P . The $P = 0$ superfluid is gapped, the FFLO has ‘pseudogaps’, *i.e.*, depression in its DOS due to the spatial modulation, while the PPFL is gapless.

2. Thermal properties:

At finite T the homogeneous SF does allow finite polarization and is called the ‘breached pair’ (BP) state¹⁵. It occupies an increasing P window, as T increases, at the expense of the unstable region. The temperature above which the SF is stable is $T_{un}(P)$. At an even higher temperature, T_{c2} , superfluidity is lost through a Berezinskii-Kosterlitz-Thouless (BKT) transition. We infer the T_c scale from $S_0(h, T)$.

The upper right edge of the unstable region defines the scale, T_{c1} , for a first order transition between the SF and the normal state. The FFLO has a very low T_c and transits to a gapless normal state on heating. This gapless phase defines a large part of the high P low temperature window.

The SF phase can be gapped or pseudogapped as Fig.1 shows, the FFLO is pseudogapped, while the PPFL is gapless at low T and pseudogapped at high T . We will discuss the origin of these behavior in the discussion section, but the phase diagram indicates that varying temperature at a fixed polarization can lead to multiple changes in spectral character. This is directly relevant for cold Fermi gases where one works at fixed imbalance rather than a fixed applied field³⁻⁵.

B. Density of states

Fig.2 shows the spin resolved DOS for fixed P cross sections through the $P - T$ phase diagram in Fig.1. Two of the panel, (a) and (d), traverse the BP part of the phase diagram, (e) starts with a FFLO ground state, while (f) has a PPFL ground state. The ground states vary widely, we discuss the cases one by one.

Fig.2(a) is for $P = 0.01$. The $T = 0$ state in this case would be in the unstable window and stable phases are defined in this case only for $T > 0.035t$. All the way from this temperature to $T_c \sim 0.17t$ the system is a BP superfluid. The behavior of the DOS, however, changes multiple times. For $0.035t < T < 0.08t$ the (shifted) DOS has its absolute minimum at $\omega = 0$ but then a local maximum at a small scale ω_{max} (see plot) and a local minimum after that at ω_{min} and then the sharp rise at the gap edge. While subgap density of states by itself is not surprising this additional feature is unusual. Increasing T beyond $\sim 0.08t$ leads to a more common PG with a monotonic increase in $N(\omega)$ as ω increases.

Fig.2(b) focuses on the low energy behavior of the data in 2(a). The lower scales clearly reveal the non monotonic DOS at low T . We fitted this behavior to an approximate form $N(\omega) = a + b\omega^2 + c\omega^4 + d\omega^6$, and, after extracting the coefficients a, b, c, d , plotted the derivative $dN/d\omega$ in Fig.2(c). The multiple zero crossings in the low T data highlight the multiple extrema.

The result in Fig.2(d) is at $P = 0.075$. The stable BP window at this P starts at $T \sim 0.07t$. Heating this BP state leads to a 2nd order transition at $T_c \sim 0.14t$. All the way from $T \sim 0.07t$ through T_c to high temperature in the PPFL phase the system is pseudogapped, with the character that we called PG-b, with monotonic $N(\omega)$. The coherence peaks vanish,

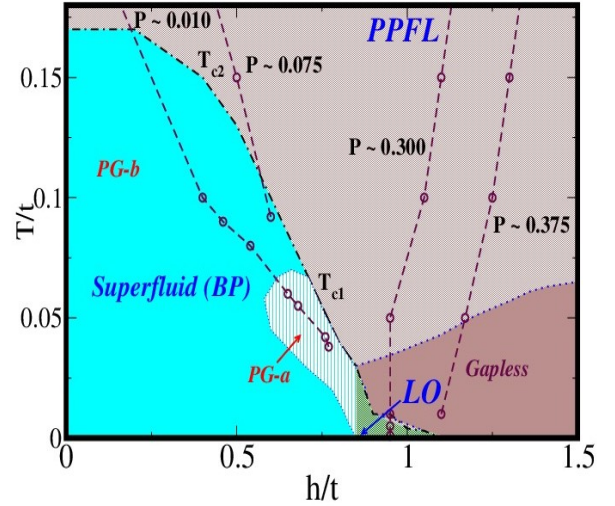


FIG. 3. Magnetic field-temperature ($h - T$) phase diagram showing the varying $h(T)$ that is needed to maintain the polarization fixed at the values chosen in Fig.2. In general when pairing effects are strong and the low T phase is a BP superfluid the magnetic field has to sharply rise with reducing T to maintain P fixed. This is clearly visible for $P = 0.01$ and weakly so for $P = 0.075$. In the higher field regime, where the low T state is FFLO or PPFL the magnetic field needs to increase somewhat with *increasing* T , as in a normal metal, to maintain a fixed P . The shaded region within the BP phase roughly correspond to the anomalous PG phase (see text for details).

the depth of the pseudogap lessens, and the low energy weight increases with increasing T .

Fig.2(e) is for $P \sim 0.30$. The ground state in this case is an axial stripe LO phase, with $\mathbf{Q} = (\pi/3, 0)$. The periodic modulation of Δ_i in the low T state leads to multiple bands and a redistribution of the tight binding spectral weight. The presence of a finite \mathbf{Q} modulation leads to pairing of fermions between $|\mathbf{k}\uparrow\rangle$ and $|\mathbf{k}\pm\mathbf{Q}\downarrow\rangle$ states (rather than the time reversed $|\mathbf{k}\uparrow\rangle$ and $|\mathbf{k}\downarrow\rangle$) and give rise to multiple branches in the dispersion. Some of these branches cross the Fermi level leading to a finite but depressed DOS around $\omega \sim 0$. This is not a fluctuation induced pseudogap but a ‘band structure’ effect. The T window immediately above T_c , $T \sim [0.01t, 0.05t]$, in Fig.2(e), is gapless. The pairing field is small and disordered and does not affect the DOS noticeably. However, at the two highest temperatures in Fig.2.(e) a weak pseudogap again emerges. This is due to the thermally induced growth in the mean magnitude $\langle|\Delta_i|\rangle$ with the phase variables θ_i remaining random. At this polarization one has a pseudogap-gapless-pseudogap re-entrance with increasing temperature.

Finally, Fig.2(f) at $P = 0.375$ has a non ordered ground state with no Δ_i at any site. This is a system at strong interaction, $U = 4t$, where the imbalance suppresses pairing at $T = 0$. As a result the low temperature phase is gapless. With increasing T the $\langle|\Delta_i|\rangle$ grows quickly, as in the FFLO window, and leads to a pseudogap for $T > 0.07t$. This is a simple instance of a pseudogap emerging without the presence of any order in the low temperature state.

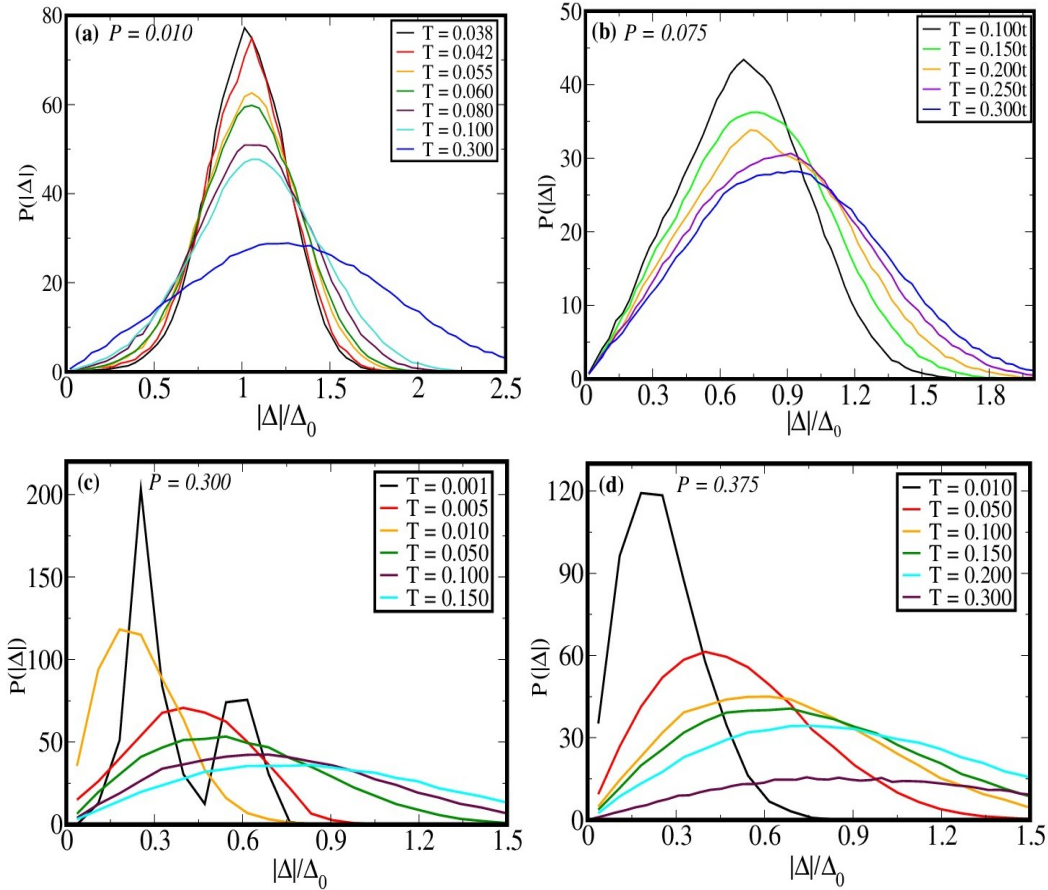


FIG. 4. The T dependence of the pairing field distribution for different P . The x axis is normalized with respect to the $T = 0$ unpolarised SF amplitude. The panels are for (a) $P \sim 0.01$, (b) $P \sim 0.075$, (c) $P \sim 0.300$ and (d) $P \sim 0.375$.

IV. DISCUSSION

We first discuss the origin of the effects seen in Fig.1 and Fig.2, and then earlier theory efforts and experimental data on this topic.

A. $h - T$ trajectory

Fig.3 shows the field-temperature phase diagram from which the $P - T$ phase diagram is derived. The basic phases have been discussed earlier in ref.¹⁵. It is included here mainly to show the rather unusual $h - T$ paths that lie behind the constant P cross sections in Fig.1.

At $P = 0.01$ the low T part of the trajectory passes close to the BP-LO phase boundary. We explored the $h - T$ neighborhood and discovered that in the window shaded grey the DOS indeed displays the peculiar features observed in Fig.2(a). The proximity to the BP-LO phase boundary, at finite T , suggests that while much of the Δ_i would have (large) values appropriate to the BP phase, there could be a small fraction of sites that have the lower values appropriate to the LO phase. We will examine this aspect in the distributions later.

The $P \sim 0.075$ trajectory transits from a high T BP phase to the PPFL. The slope of the $h(T)$ curve is much smaller than for $P = 0.01$ due to the weaker suppression of Pauli susceptibility. The $P \sim 0.30$ system passes from a low T LO phase to a PPFL, while the $P \sim 0.375$ path is always in an unordered phase but displays a high T pseudogap due to thermal fluctuations. For these two cases, where the ground state does not have Pauli susceptibility suppression, the $h(T)$ curves generally have a weak positive slope. In this window the ‘mysterious’ effect is the presence of a high T pseudogap above a gapless low temperature state. Addressing this requires a look at the pairing field distributions.

B. Pairing field distribution

Fig.4 shows the distribution of the pairing field for the different fixed P cross sections shown in Fig.2. Fig.4.(a) shows the pairing field distributions for DOS shown in Fig.2.(a), and so on for the other panels.

The anomalous low energy features in Fig.2(a), we believe, arise from the relatively large number of *small* Δ_i sites in a typical configuration in this part of parameter space. This arises due to the proximity to the low Δ FFLO state. While the

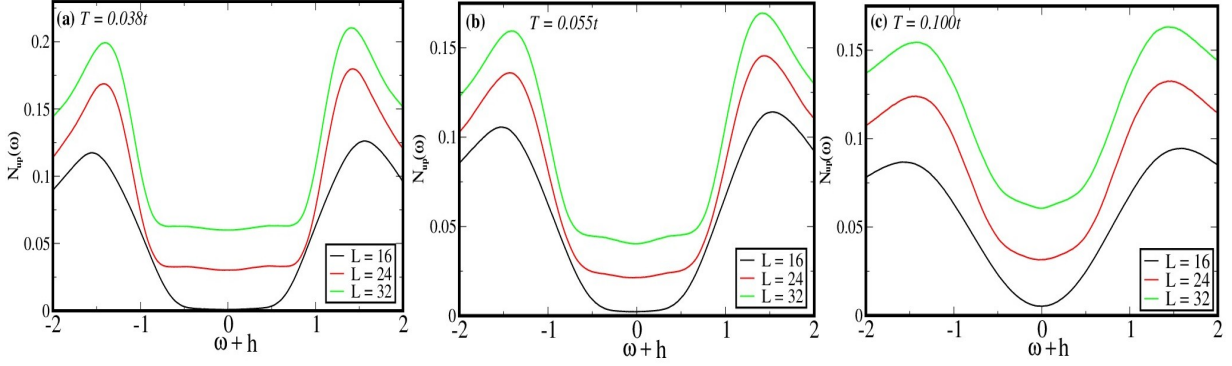


FIG. 5. Size dependence of the DOS at a polarization $P = 0.01$ and three temperatures. The curves are y shifted by equal amounts for clarity. We observe that (i) $L = 24$ and $L = 32$ results are quite similar (and different from $L = 16$), and (ii) the DOS at low temperature, panels (a) and (b), have a consistent non monotonic low energy feature.

mean Δ is $\sim \Delta_0$ (the $T = 0$ mean field value), at $T \sim 0.04t$ in Fig.4(a), if the system were fully in the LO regime, Fig.4(c), the mean Δ would be $\sim 0.5\Delta_0$, see the plot for $T = 0.05t$. We think that proximity to the LO phase boundary makes the system have a small fraction of small Δ sites whose magnitude is ~ 0.5 the typical value. As a result the DOS generates weight at an energy ω_{max} that is roughly 0.5 the gap edge value. Since the $P = 0.01$ trajectory is the only one that borders the BP-LO boundary the effect is not visible at other P .

Fig.4.(b) shows a monotonic increase in the width of $P(|\Delta_i|)$ with increasing T , and the increasing ‘disorder’ in the pairing field steadily weakens the PG in the DOS and increases the low energy spectral weight. In Fig.4.(c) the lowest T shows the ‘multimode’ distribution of the amplitude modulated LO state. At this, and the next higher T , the LO modulations lead to a ‘pseudogapped’ phase but with the loss of order at the first order transition, $T \sim 0.005t$, the mean amplitude collapses. A gapless state emerges, and survives to some larger temperature, where the thermal fluctuations have created enough large Δ_i sites to generate a weak pseudogap. The behavior in 4.(d) is essentially similar to 4.(c), with the LO part removed: in this case one just has a gapless to weak PG crossover.

C. Earlier work

Much of the earlier work on pseudogaps in imbalanced superfluids is in the continuum context. A *thermodynamic re-entrance* has been pointed out in the continuum unitary gas^{9,10} at low P . The authors there had carried out an extensive investigation in terms of interaction strength ($1/k_F a$), polarization, and temperature and observed that near $1/k_F a = 0$ the low P superfluid state has an upper and lower bound in temperature^{9,10,20}. At $T = 0$ there is no stable superfluid, while an intermediate SF phase is realized at $T \neq 0$. The superfluid is gapped (by construction in this theory) the higher and lower T ‘normal’ states are pseudogapped. The present theory allows for pairing field fluctuations, consequently we find that within the SF phase the spectrum is not always

gapped out completely and there are finite low energy weight even at the lowest accessible temperature. Despite the different model, a quite different approximation, and a thermodynamic stability (rather than spectral change) argument offered by the authors, we think the similarity with our result is not coincidental. The changing spectral character at the small polarization regime bears closer experimental search.

The spectrum in imbalanced superconductors can be probed by tunneling but we are not aware of such studies. Spectral studies are more visible in cold atomic superfluids, although the results are complicated by the effect of a trap. The experiments measure a ‘radio frequency’ (RF) current^{21–23}, rather than the density of states. However, the RF response $I_\sigma(\omega)$ is a weighted sum^{24,25} of the same spectral function $A_\sigma(\mathbf{k}, \omega) = -(1/\pi)ImG_\sigma(\mathbf{k}, \omega)$ that defines our density of states $N_\sigma(\omega)$.

Experiments on the unitary Fermi gas indicate that the T_c falls from $\sim 0.2T_F$ at $P = 0$ to zero at $P_c \sim 0.75$. The ‘pair formation’ scale T_{pair} , however, seems to be $\mathcal{O}(T_F)$ even when P crosses P_c and T_c falls to zero¹³. These experiments suggest that a PG is obtained over a wide temperature window all the way from $P = 0$ to the highest P . Our results agree with this, except at the high P end where we observe a gapless low temperature state. This difference arises from our neglect of quantum fluctuations in the $\Delta_i(\tau)$, which can generate a non trivial Fermi liquid ground state^{24,25}, preserving pairing but suppressing condensation.

D. Finite size effect

The results discussed in this paper correspond to a lattice size of $L = 32$. The system size is reasonable in comparison to the existing literature in which the thermal physics of spin imbalanced system are being explored²⁶. In order to verify the robustness of the spectral features, we have further computed our results on various other system sizes. Fig.(5) shows the spin resolved DOS calculated at three different lattice sizes of $L = 16, 24$ and 32 , for a fixed polarization, highlighting three different temperature regimes. We observed that the anoma-

lous behavior of the spin resolved DOS is fairly robust and persists even at $L = 24$, and is not an artifact of finite size effect.

V. CONCLUSION

We have established the thermal phase diagram of population imbalanced lattice fermions near the BCS-BEC crossover and observed that although the thermodynamic phases exhibit expected behavior with temperature the spectral features are very counter-intuitive. The low temperature superfluid at a fixed small polarization has a pseudogap with a distinct max-

imum in the density of states in the subgap region, crossing over to a more conventional featureless pseudogap with increasing temperature. The unusual low (but finite) temperature result arises due to LO like fluctuations in the BP phase near the BP-LO boundary. At large polarization, in the LO phase, the system undergoes a pseudogap to gapless to pseudogap crossover with increasing temperature, At even larger polarization, where the ground state is gapless and has no pairing and long range order, heating the system leads to pseudogap formation above a certain temperature. All these effects are a consequence of thermal fluctuations beyond the mean field scheme usually used to analyze these models.

We acknowledge use of the HPC clusters at HRI and thank Nyayabanta Swain for comments.

-
- ¹ M. Randeria, Nat. Phys. **6**, 561 (2010).
² K. Kumagai, M. Saitoh, T. Oyaizu, Y. Furukawa, S. Takashima, M. Nohara, H. Takagi and Y. Matsuda, Phys. Rev. Lett. **97**, 227002 (2006).
³ Y. -il Shin, C. H. Schunck, A. Schirotzek and W. Ketterle, Nature **451**, 689 (2008).
⁴ G. B. Partridge, W. Li, R. I. Kamar, Y.-an Liao, R. G. Hulet, Science **311**, 503 (2006).
⁵ Y. -an Liao, A. S. C. Rittner, T. Paprotta, W. Li, G. B. Partridge, R. G. Hulet, S. K. Baur and E. J. Mueller, Nature **467**, 567 (2010).
⁶ P. Fulde and R. A. Ferrell, Phys. Rev. **135**, A550 (1964).
⁷ A. I. Larkin and Yu. N. Ovchinnikov, Zh. Eksp. Teor. Fiz. **47**, 1136 (1964); Sov. Phys. JETP **20**, 762 (1965).
⁸ G. Sarma, J. Phys. Chem. Solids **24**, 1029 (1963).
⁹ C. Ch. Chien, Q. Chen, Y. He and K. Levin, Phys. Rev. Lett. **97**, 090402 (2006).
¹⁰ Q. Chen, Y. He, C. Ch. Chien and K. Levin, Phys. Rev. A **74**, 063603 (2006).
¹¹ T. K. Koponen, T. Paananen, J. -P. Martikainen and P. Torma, Phys. Rev. Lett. **99**, 120403 (2007).
¹² M. O. J. Heikkinen, D. H. Kim and P. Torma, Phys. Rev. B **87**, 224513 (2013).
¹³ C. H. Schunck, Y. Shin, A. Schirotzek, M. W. Zwierlein and W. Ketterle, Science **316**, 867 (2007).
¹⁴ S. Tarat and P. Majumdar, Eur. Phys. J. B **88**, 68 (2015).
¹⁵ M. Karmakar and P. Majumdar, arXiv: 1508:00393.
¹⁶ W. E. Evenson, J. R. Schrieffer and S. Q. Wang, J. Appl. Phys. **41**, 1199 (1970).
¹⁷ J. Hubbard, Phys. Rev. B **19**, 2626 (1979).
¹⁸ S. Kumar and P. Majumdar, Eur. Phys. J. B **50**, 571 (2006).
¹⁹ P. J. de Gennes, *Superconductivity of metals and alloys*, (1999).
²⁰ W. Yi and L. M. Duan, Phys. Rev. A **73**, 031604(R) (2006); A. Sedrakian and U. Lombardo, Phys. Rev. Lett. **84**, 602 (2000).
²¹ Y. Shin, C. H. Schunck, A. Schirotzek and W. Ketterle, Phys. Rev. Lett. **99**, 090403 (2007).
²² C. Chin, M. Bartenstein, A. Altmeyer, S. Riedl, S. Jochim, J. H. Denschlag and R. Grimm, Science **305**, 1128 (2004).
²³ A. Schirotzek, Y. Shin, C. H. Schunck and W. Ketterle, Phys. Rev. Lett. **101**, 140403 (2008).
²⁴ M. Veillette, E. G. Moon, A. Lamacraft, L. Radzihovsky, S. Sachdev, and D. E. Sheehy, Phys. Rev. A **78**, 033614 (2008).
²⁵ Y. He, C-Ch. Chien, Q. Chen and K. Levin, Phys. Rev. A **77**, 011602 (2008).
²⁶ M. J. Wolak, B. Gremaud, R. T. Scalettar and G. G. Batrouni, Phys. Rev. A **86**, 023630 (2012).